

Solar Flares and the Axion Quark Nugget Dark Matter Model

Ariel Zhitnitsky

Department of Physics & Astronomy, University of British Columbia, Vancouver, B.C. V6T 1Z1, Canada

Abstract. We advocate the idea that the nanoflares conjectured by Parker long ago to resolve the corona heating problem, may also trigger the larger solar flares. The arguments are based on the model where emission of extreme ultra violet (EUV) radiation and soft x-rays from the Sun are powered externally by incident dark matter particles within the Axion Quark Nugget (AQN) Dark Matter Model. The corresponding annihilation events of the AQNs with the solar material are identified with nanoflares. This model was originally invented as a natural explanation of the observed ratio $\Omega_{\text{dark}} \sim \Omega_{\text{visible}}$ when the DM and visible matter densities assume the same order of magnitude values. This model gives a very reasonable intensity of EUV radiation without adjustments of any parameters in the model. When the same nuggets enter the regions with high magnetic field they serve as the triggers igniting the magnetic reconnections which eventually may lead to much larger flares.

Technically, the magnetic reconnection is ignited due to the shock wave which inevitably develops when the dark matter nuggets enter the solar atmosphere with velocity $v \sim 10^{-3}c$ which is much higher than the speed of sound c_s , such that the Mach number $M = v/c_s \gg 1$. These shock waves generate very strong and very short impulses expressed in terms of pressure $\Delta p/p \sim M^2$ and temperature $\Delta T/T \sim M^2$ in vicinity of (would be) magnetic reconnection area. We find that this mechanism is consistent with x-ray observations as well as with observed jet like morphology of the initial stage of the flares. The mechanism is also consistent with the observed scaling of the flare distribution $dN \sim W^{-\alpha}dW$ as a function of the flare's energy W . We also speculate that the same nuggets may trigger the sunquakes which are known to be correlated with large flares.

Contents

1	Introduction	1
2	Axion Quark Nugget (AQN) dark matter model	4
3	The AQN annihilation events as nanoflares	7
3.1	Energetic budget due to the AQN annihilation events	7
3.2	Observation of nanoflares as evidence for anti-nuggets in Corona	8
3.3	From nanoflares \Rightarrow microflares \Rightarrow large solar flares	10
4	AQNs as the triggers initiating the solar flares	11
4.1	Magnetic reconnection and Sweet-Parker theory	12
4.2	AQNs and shock waves in plasma	12
4.3	Magnetic reconnection ignited by the shock waves	14
4.4	Geometrical interpretation of the scaling $dN \sim W^{-\alpha} dW$	17
5	AQNs as triggers of solar flares: proposal confronting the observations	19
5.1	Pre-flare x-ray radiation: intensity, timing and direction of the flare propagation (from top to bottom)	19
5.2	Shapes of the anemone jets	20
5.3	Other related phenomena: sunquakes	21
6	Conclusion and final remarks	22

1 Introduction

A variety of anomalous solar phenomena still defy conventional theoretical understanding. For example, the detailed physical processes that heat the outer atmosphere of the Sun to 10^6K remain a major open issue in astrophysics, see e.g. [1] for review and references on the original results. This persisting puzzle is characterized by the following observed anomalous behaviour of the sun: the quiet Sun emits an extreme ultra violet (EUV) radiation with a photon energy of order of hundreds of eV which cannot be explained in terms of any conventional astrophysical phenomena; the total energy output of the corona is quite small, see (1.1) below. However, it never drops to zero as time evolves. To be more specific, the total intensity of the observed EUV and soft x-ray radiation (averaged over time) can be estimated as follows,

$$L_{\odot} \text{ (from Corona)} \sim 10^{30} \cdot \frac{\text{GeV}}{\text{s}} \sim 10^{27} \cdot \frac{\text{erg}}{\text{s}}. \quad (1.1)$$

which represents about $(10^{-7} - 10^{-6})$ fraction of the solar luminosity.

At the transition region, the (quiet Sun) temperature continues to rise very steeply until it reaches a few 10^6 K, i.e., being a few 100 times hotter above the underlying photosphere, and this within an atmospheric layer thickness of only 100 km or even much less. Therefore, after several decades of research, it may be that the answer on these (and many others related) questions lies in a new physics.

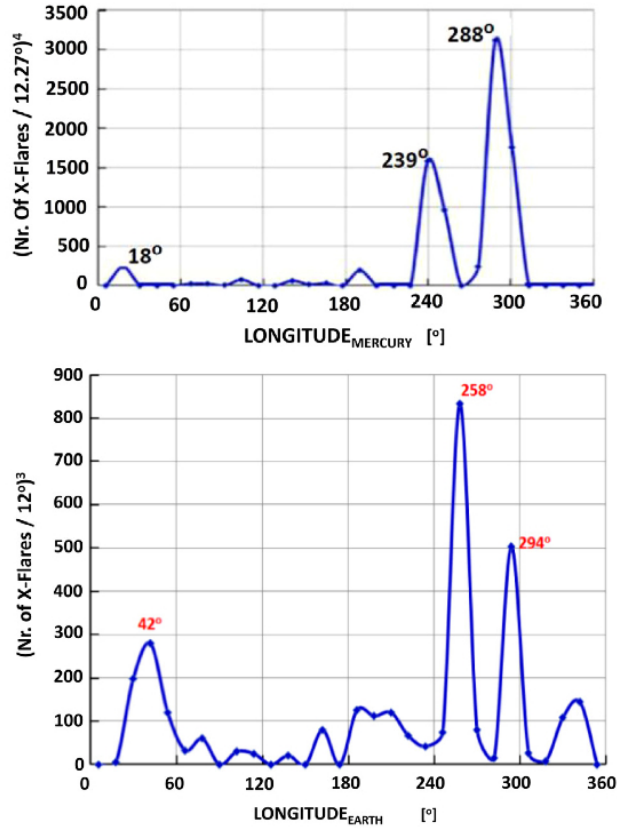


Figure 1. The “multiplication spectrum” is defined as $Y(J) \equiv \Theta_1(J) \cdot \Theta_2(J) \cdot \Theta_3(J) \cdot \Theta_4(J)$, where Θ is the deflection angle related to the gravitational lensing analysis. The subscript (1-4) denotes the four solar cycles (1975-1986, 1986-1997, 1997-2009, 2009-2014) and J denotes the bin number with widths ($6^\circ, 12^\circ, 16^\circ$). The plots are taken from [2].

It was precisely the main subject of ref.[2] where it was advocated that a number of highly unusual phenomena (including, but not limited to the EUV radiation) observed in solar atmosphere might be related to the gravitational lensing of “invisible” streaming matter towards the Sun. The main argument of ref.[2] is based on analysis of a number of different correlations between the relative orientations of the Sun and its planets on the one hand and the frequency of the observed flares on the other hand of the analysis. As an example of the observed correlations we reproduce on Fig.1 some sample plots for the so-called “multiplication spectrum” from ref. [2] where the frequency of occurring of the X-flares is shown as a function of the Mercury (on the top) and the Earth (on the bottom) heliocentric longitude. We refer to the original paper [2] for the specific discussions, definitions and the details on the data analysis. In this Introduction the only comment we would like to make is that one should not expect any correlations between the X flare occurrences and the position of the planets. Nevertheless, Fig.1 obviously demonstrates that this naive expectation is not quite correct, and that the enhancement is happening around the same heliocentric longitude for Mercury and Earth in spite of the fact that periods of the Earth and Mercury are very different ($T_{\text{Mercury}} = 87.969$ days) and they appear at this specific heliocentric longitude when the enhancement occurs, in general, at different moments.

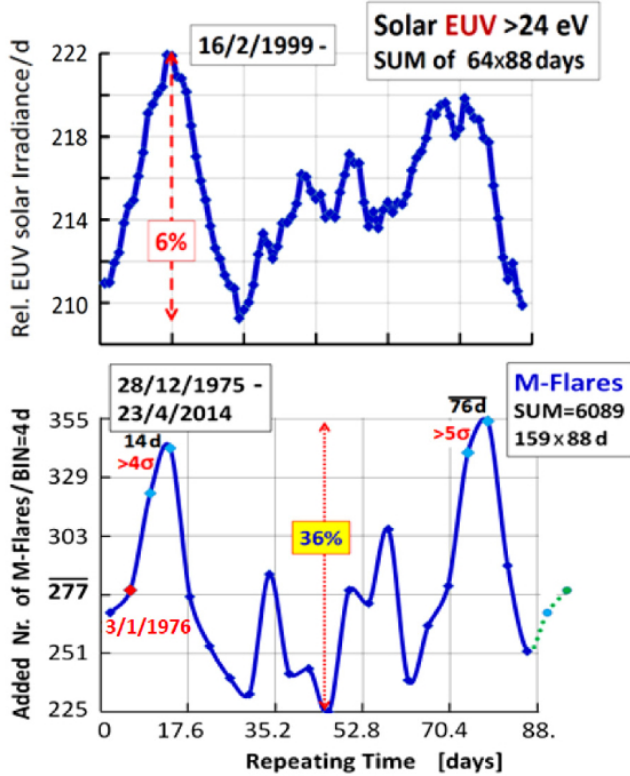


Figure 2. This plot demonstrates the correlation between the relative EUV radiation (top) and the number of M-flares during the same period of time (bottom). The BIN size is 1 day for the EUV data and 4 days for M-flares analysis. The plots are taken from [2].

In recent paper [3] this idea (on correlation of the solar activity with position of its planets) has received some analytical and numerical support by offering an explicit realization of the “invisible matter” conjectured in [2] in form of a very specific dark matter model, the so-called the axion quark nugget (AQN) dark matter model. It has been argued in [3] that the dark matter AQNs might be the source of the heating of outer atmosphere of the Sun and, therefore, might be directly responsible for the observed EUV radiation. One should emphasize that the AQN dark matter model was originally proposed long ago [4] without any connection to the solar system and the EUV. Rather, the main motivation to develop the AQN dark matter model was to explain in a very natural way the observed similarity between the visible and dark matter densities in the present Universe, i.e. $\Omega_{\text{dark}} \sim \Omega_{\text{visible}}$, see short overview of the AQN model in the next section 2.

It turns out that if one estimates the extra energy being produced within the AQN dark matter scenario one obtains the total extra energy $\sim 10^{27}$ erg/s which precisely reproduces (1.1) for the observed EUV and soft x-ray intensities [3]. One should emphasize that this estimation for extra energy is expressed exclusively in terms of known dark matter density $\rho_{\text{DM}} \sim 0.3 \text{ GeVcm}^{-3}$ and dark matter velocity $v_{\text{DM}} \sim 10^{-3}c$ surrounding the Sun without adjusting any parameters of the AQN model, see section 3 below with relevant comments. We interpreted this “numerical coincidence” in [3] as an additional argument supporting our

proposal that the heating of the corona and the chromosphere is originated from the AQNs entering the solar atmosphere from outer space.

The present work is largely motivated by the observation made in [2] that the EUV emission from the corona is strongly correlated with occurrences of the X, M flares, as shown in Fig.2. At the same time, as we mentioned above, the intensity and spectral properties of the EUV emission can be understood within the AQN scenario as argued in [3]. A strong correlation between the EUV radiation and occurrences of the X, M flares unambiguously suggests that these two apparently distinct phenomena in fact intimately linked as they obviously accompany each other according to Fig.2.

The main purpose of the present work is to present a very specific mechanism which explicitly shows how these two naively distinct phenomena nevertheless closely related to each other. This deep relation between these two distinct effects may shed some light on the nature of the dark matter which (within the AQN paradigm) is the source for both phenomena, the EUV radiation and the flare's activity.

The paper is organized as follows. In next section 2 we overview the AQN model by paying special attention to the astrophysical and cosmological consequences of this specific dark matter model. In section 3 we highlight the basic arguments of ref. [3] advocating the idea that the annihilation events of the antinuggets with the solar material can be interpreted as the *nanoflares* conjectured by Parker long ago. In the section 4 we argue that the same AQNs entering the region with the large magnetic field may spark the magnetic reconnection leading to very large *flares*. In other words, we want to argue that the AQNs may play the role of the *triggers* initiating the large scale flares in the regions with large magnetic field. To be more specific, we want to argue that the shock waves (which will be always generated as a result of high velocity of the dark matter nuggets entering the Sun with $v \sim 10^{-3}c$ which is much greater than the speed of sound c_s) can easily initiate the large flares as a result of the magnetic reconnection. In section 5 we review some observations, including x-ray data and morphology (anemone jets) supporting the basic framework. We also speculate that the sunquakes might be also related to the same AQNs initially entering from outer space and capable to reach the photospheric layer.

2 Axion Quark Nugget (AQN) dark matter model

The AQN model in the title of this section stands for the axion quark nugget model, see original work [4] and short overview [5] with large number of references on the original results reflecting different aspects of the AQN model. In comparison with many other similar proposals it has two unique features:

1. There is an additional stabilization factor in the AQN model provided by the *axion domain walls* which are copiously produced during the QCD transition in early Universe;
2. The AQNs could be made of matter as well as *antimatter* in this framework as a result of separation of the baryon charges.

The most important astrophysical implication of these new aspects relevant for the present studies (focusing on different types of flares and sources of the EUV and x-ray radiation in the solar chromosphere and corona) is that quark nuggets made of antimatter store a huge amount of energy which can be released when the anti-nuggets hit the Sun from outer space and get annihilated. This feature of the AQN model is unique and is not shared by any other dark matter models because the dark matter in AQN model is made of the same quarks and antiquarks of the standard model (SM) of particle physics. One should also remark here

that the annihilation events of the anti-nuggets with visible matter may produce a number of other observable effects in different circumstances such as rare events of annihilation of anti-nuggets with visible matter in the centre of galaxy, or in the Earth atmosphere, see some references on the original computations in [5] and few comments at the end of this section.

The basic idea of the AQN proposal can be explained as follows: It is commonly assumed that the Universe began in a symmetric state with zero global baryonic charge and later (through some baryon number violating process, the so-called baryogenesis) evolved into a state with a net positive baryon number. As an alternative to this scenario we advocate a model in which “baryogenesis” is actually a charge separation process when the global baryon number of the Universe remains zero. In this model the unobserved antibaryons come to comprise the dark matter in the form of dense nuggets of quarks and antiquarks in colour superconducting (CS) phase. The formation of the nuggets made of matter and antimatter occurs through the dynamics of shrinking axion domain walls, see original papers [6, 7] with many technical details.

The nuggets, after they formed, can be viewed as the strongly interacting and macroscopically large objects with a typical nuclear density and with a typical size $R \sim (10^{-5} - 10^{-4})\text{cm}$ determined by the axion mass m_a as these two parameters are linked, $R \sim m_a^{-1}$. This relation between the size of nugget R and the axion mass m_a is a result of the equilibration between the axion domain wall pressure and the Fermi pressure of the dense quark matter in CS phase. One can easily estimate a typical baryon charge B of such macroscopically large objects as the typical density of matter in CS phase is only few times the nuclear density. However, it is important to emphasize that there are strong constraints on the allowed window for the axion mass, which can be represented as follows $10^{-6}\text{eV} \leq m_a \leq 10^{-2}\text{eV}$, see original papers [8–10] and reviews [11–18] on the theory of the axion and recent progress on axion search experiments.

This axion window corresponds to the range of the nugget’s baryon charge B which largely overlaps with all presently available and independent constraints on such kind of dark matter masses and baryon charges

$$10^{23} \leq |B| \leq 10^{28}, \quad (2.1)$$

see e.g. [5, 19] for review¹. The corresponding mass M of the nuggets can be estimated as $M \sim m_p B$, where m_p is the proton mass, though more precise estimates relating the axion mass m_a , the baryon nuggets charge B and the baryon mass M are also available [20].

This model is perfectly consistent with all known astrophysical, cosmological, satellite and ground based constraints within the parametrical range for the mass M and the baryon charge B mentioned above (2.1). It is also consistent with known constraints from the axion search experiments. Furthermore, there is a number of frequency bands where some excess of emission was observed, but not explained by conventional astrophysical sources. Our comment here is that this model may explain some portion, or even entire excess of the

¹The smallest nuggets with $B \sim (10^{23} - 10^{24})$ naively contradict to the constraints cited in [19]. However, the corresponding constraints are actually derived with the assumption that nuggets with a definite mass (smaller than 55g) saturate the dark matter density. In contrast, we assume that the peak of the nugget’s distribution corresponds to a larger value of mass, $\langle B \rangle \geq 10^{25}$, while the small nuggets represent a tiny portion of the total dark matter density. The same comment also applies to the larger masses excluded by Apollo data as reviewed in [5]. Large nuggets with $B \sim 10^{28}$ may exist, but represent a small portion of the total dark matter density, and therefore, do not contradict the Apollo’s constraints, see also some comments on the baryon charge distribution (3.5) in section 3.

observed radiation in these frequency bands, see short review [5] and additional references at the end of this section.

Another key element of this model is the coherent axion field θ which is assumed to be non-zero during the QCD transition in early Universe. As a result of these \mathcal{CP} violating processes the number of nuggets and anti-nuggets being formed would be different. This difference is always of order of one effect [6, 7] irrespectively to the parameters of the theory, the axion mass m_a or the initial misalignment angle θ_0 . As a result of this disparity between nuggets and anti nuggets a similar disparity would also emerge between visible quarks and antiquarks. This is precisely the reason why the resulting visible and dark matter densities must be the same order of magnitude [6, 7]

$$\Omega_{\text{dark}} \sim \Omega_{\text{visible}} \quad (2.2)$$

as they are both proportional to the same fundamental Λ_{QCD} scale, and they both are originated at the same QCD epoch. If these processes are not fundamentally related the two components Ω_{dark} and Ω_{visible} could easily exist at vastly different scales.

Unlike conventional dark matter candidates, such as WIMPs (Weakly interacting Massive Particles) the dark-matter/antimatter nuggets are strongly interacting and macroscopically large objects, as we already mentioned. However, they do not contradict any of the many known observational constraints on dark matter or antimatter in the Universe due to the following main reasons [21]: They carry very large baryon charge $|B| \gtrsim 10^{23}$, and so their number density is very small $\sim B^{-1}$. As a result of this unique feature, their interaction with visible matter is highly inefficient, and therefore, the nuggets are perfectly qualify as DM candidates. Furthermore, the quark nuggets have very large binding energy due to the large gap $\Delta \sim 100$ MeV in CS phases. Therefore, the baryon charge is so strongly bounded in the core of the nugget that it is not available to participate in big bang nucleosynthesis (BBN) at $T \approx 1$ MeV, long after the nuggets had been formed.

It should be noted that the galactic spectrum contains several excesses of diffuse emission the origin of which is unknown, the best known example being the strong galactic 511 keV line. If the nuggets have the average baryon number in the $\langle B \rangle \sim 10^{25}$ range they could offer a potential explanation for several of these diffuse components. It is important to emphasize that a comparison between emissions with drastically different frequencies in such computations is possible because the rate of annihilation events (between visible matter and antimatter DM nuggets) is proportional to one and the same product of the local visible and DM distributions at the annihilation site. The observed fluxes for different emissions thus depend through one and the same line-of-sight integral

$$\Phi \sim R^2 \int d\Omega dl [n_{\text{visible}}(l) \cdot n_{DM}(l)], \quad (2.3)$$

where $R \sim B^{1/3}$ is a typical size of the nugget which determines the effective cross section of interaction between DM and visible matter. As $n_{DM} \sim B^{-1}$ the effective interaction is strongly suppressed $\sim B^{-1/3}$. The parameter $\langle B \rangle \sim 10^{25}$ was fixed in this proposal by assuming that this mechanism saturates the observed 511 keV line [22, 23], which resulted from annihilation of the electrons from visible matter and positrons from anti-nuggets. Other emissions from different frequency bands are expressed in terms of the same integral (2.3), and therefore, the relative intensities are unambiguously and completely determined by internal structure of the nuggets which is described by conventional nuclear physics and basic QED, see short overview [5] with references on specific computations of diffuse galactic radiation in different frequency bands.

3 The AQN annihilation events as nanoflares

We start our overview of the basic results of ref [3] with subsection 3.1 where we present simple estimates of the energetic budget suggesting that the heating of the chromosphere and corona might be due to the annihilation events of the AQN with the solar material. As the next step, in subsection 3.2 we highlight the arguments of ref. [3] suggesting that the corresponding annihilation events heating the corona can be identified with the nanoflares conjectured by Parker long ago [24]. Finally, in subsection 3.3 we describe some recent observations of microflares and flares (along with nanoflares) suggesting that all these phenomena might be in fact tightly connected and originated from the same AQNs in spite of the fact that these phenomena are characterized by drastically different energy scales: from 10^{20} erg for nanoflares (much below the instrumental threshold being $\sim 10^{24}$ erg) to 10^{32} erg for largest solar flares.

We elaborate on this proposal in the following section 4 by demonstrating that the shock waves will be always generated as a result of very high velocity of the AQNs entering the Sun with $v \simeq 10^{-3}c$. These shock waves may serve as the triggers initiating the large solar flares if the AQNs enter the region of high magnetic field in which case the AQNs may activate the magnetic reconnection of *preexisted* magnetic fluxes.

3.1 Energetic budget due to the AQN annihilation events

The impact parameter for capture of the nuggets by the Sun can be estimated as

$$b_{\text{cap}} \simeq R_{\odot} \sqrt{1 + \gamma_{\odot}}, \quad \gamma_{\odot} \equiv \frac{2GM_{\odot}}{R_{\odot}v^2}, \quad (3.1)$$

where $v \simeq 10^{-3}c$ is a typical velocity of the nuggets. One can easily see that $\gamma_{\odot} \gg 1$ which implies that many AQNs which are not on head on collision trajectory, nevertheless will be eventually captured by the Sun. Nuggets in the solar atmosphere will be decreasing their mass as result of annihilation, decreasing their kinetic energy and velocity as result of ionization and radiation.

Assuming that $\rho_{\text{DM}} \sim 0.3 \text{ GeVcm}^{-3}$ and using the capture impact parameter (3.1), one can estimate the total energy flux due to the complete annihilation of the nuggets,

$$L_{\odot} (\text{AQN}) \sim 4\pi b_{\text{cap}}^2 \cdot v \cdot \rho_{\text{DM}} \simeq 3 \cdot 10^{30} \cdot \frac{\text{GeV}}{\text{s}} \simeq 4.8 \cdot 10^{27} \cdot \frac{\text{erg}}{\text{s}}, \quad (3.2)$$

where we substitute constant $v \simeq 10^{-3}c$ to simplify numerical analysis. This estimate is very suggestive as it roughly coincides with the total EUV energy output (1.1) from corona which is hard to explain in terms of conventional astrophysical sources as highlighted in the Introduction. Precisely this ‘‘accidental numerical coincidence’’ was the main motivation to put forward the idea [3] that (3.2) represents a new source of energy feeding the EUV and x-ray radiation.

The main assumption made in [3] is that a finite portion of annihilation events have occurred before the anti-nuggets entered the dense regions of the Sun. Just these annihilation events supply the energy source of the observed EUV and x-ray radiation from the corona and the chromosphere. The crucial observation made in [3] is that while the total energy due to the annihilation of the anti-nuggets is indeed very small as it represents $\sim 10^{-6}$ fraction of the solar luminosity according to (1.1), nevertheless the anti-nuggets produce the EUV

and x-ray spectrum characterized by the temperature $T \sim 10^6\text{K}$. Such spectrum observed in corona and the chromosphere is hard to explain by any conventional astrophysical processes as mentioned in the Introduction.

One should emphasize that the estimates (3.2) for the total intensity as well as the estimate for a typical temperature $T \sim 10^6\text{K}$ are not sensitive to the size distribution of the nuggets. This is because the estimate (3.2) represents the total energy input due to the complete nugget's annihilation, while their total baryon charge is determined by the dark matter density $\rho_{\text{DM}} \sim 0.3 \text{ GeVcm}^{-3}$ surrounding the Sun.

3.2 Observation of nanoflares as evidence for anti-nuggets in Corona

In this subsection we highlight the arguments of ref. [3] where the annihilation events of the anti-nuggets, which generate the energy (3.2), are identified with the previously studied "nanoflares", which belong to the burst-like solar activity. The term "nanoflare" has been introduced by Parker in 1983 [24]. Later on this term has been used in series of papers by Benz and coauthors [25–29] and many others to advocate the idea that precisely these small "micro-events" might be responsible for the heating of the quiet solar corona. It is not the goal of this work to review different aspects and different analyses related to the nanoflares and the heating mechanisms. Instead, we just want to mention few papers on relatively recent studies [30–33] and reviews [1, 34] which support the basic claim of early works that the nanoflares play the dominate role in heating of solar corona. However, some disagreement still remains between different groups on spectral properties of the nanoflares, see some details below.

We start this overview by providing the relation between the energy of the flares and the baryon charge B of the AQNs. Annihilation of a single baryon charge produces the energy about 2 GeV which is convenient to express in terms of the conventional units as follows,

$$1 \text{ GeV} = 1.6 \cdot 10^{-10} \text{ J} = 1.6 \cdot 10^{-3} \text{ erg.} \quad (3.3)$$

In particular, this relation implies that the current instrumental threshold of a nanoflare characterized by the energy $\sim 10^{24}$ erg corresponds to the (anti) baryon charge of the nugget $B \approx 3 \cdot 10^{26}$ which falls to the window (2.1) of the allowed baryon charges for the AQNs. The nanoflares with sub-resolution energies (corresponding to smaller values of B) must be present in the corona to reproduce the measured radiation loss, but are considered to be the sub-resolution events, and cannot be resolved by the presently available instruments.

Before we proceed with the arguments [3] suggesting that the nanoflares can be interpreted as the annihilation events of the AQNs with the solar material, we would like to make few comments on the modern definitions of the nanoflares. In most studies the term "nanoflare" describes a generic event for any impulsive energy release on a small scale, without specifying its cause. In other words, in most studies the hydrodynamic consequences of impulsive heating (due to the nanoflares) have been used without discussing their nature, see review papers [1, 34]. The definition suggested in [29] is essentially equivalent to the definition adopted in [1, 34] and refers to nanoflares as the "micro-events" in quiet regions of the corona, to be contrasted with "microflares" which are significantly larger in scale and observed in active regions. The term "micro-events" refers to a short enhancement of coronal emission in the energy range of about $(10^{24} - 10^{28})$ erg when the lower limit gives the instrumental threshold observing quiet regions, while the upper limit refers to the smallest events observable in active regions.

With these preliminary comments on definitions and units we want to highlight below few important features which have been discussed in previous works [25–29]. We also want

to show how these features are realized within the AQN framework [3] advocating the idea that these nanoflares have the same properties as annihilation events of antinuggets in the corona. Therefore, the proposal of [3] is to identify them, i.e.

$$\text{nanoflares} \equiv \text{AQN annihilation events.} \quad (3.4)$$

First of all, according to ref.[27] to reproduce the measured radiation loss, the observed range of nanoflares needs to be extrapolated from sub-resolution events with energy $3.7 \cdot 10^{20}$ erg to the observed events interpolating between $(3.1 \cdot 10^{24} - 1.3 \cdot 10^{26})$ erg. This energy window corresponds to the (anti)baryon charge of the nugget $10^{23} \leq |B| \leq 4 \cdot 10^{28}$ which largely overlaps with allowed window (2.1) for AQNs reviewed in section 2. We want to emphasize that this is a highly nontrivial consistency check for the proposal (3.4) as the window (2.1) comes from a number of different and independent constraints extracted from astrophysical, cosmological, satellite and ground based observations. The window (2.1) is also consistent with known constraints from the axion search experiments within the AQN framework. Therefore, the overlap between these two fundamentally different entities represents a highly nontrivial consistency check of the proposal (3.4).

Our next comment goes as follows. According to ref.[29] the nanoflares are distributed very *uniformly in quiet regions*, in contrast with micro-flares which are much more energetic and occur exclusively in active areas. It is perfectly consistent with our identification (3.4) as the anti-nugget annihilation events should be present in all areas irrespectively to the activity of the Sun. At the same time the micro- flares are originated in the active zones, and therefore cannot be uniformly distributed.

Our next comment is related to the observation of the large Doppler shift with a typical velocities (250-310) km/s, see Fig.5 in ref. [25]. Furthermore, the observed line width in OV of ± 140 km/s far exceeds the thermal ion velocity which is around 11 km/s [25]. These observed features can be easily understood within the AQN framework and its identification proposal (3.4). Indeed, the typical velocities of the nuggets entering the solar corona is about ~ 300 km/s. Therefore, it is perfectly consistent with observations of the very large Doppler shifts and related broadenings of the line widths. Typical time-scales of the nanoflare events, of order of $(10^1 - 10^2)$ sec. are also consistent with estimates [3].

One should also remark here that the energy output observed by EIT on the SoHO satellite is of order of 10% of the total radiative output in the same region [28]. The interpretation of this ‘‘apparent deficiency’’ is very straightforward within our identification (3.4). Indeed, only a small portion of the AQNs are sufficiently large to produce the events with the energies above the instrumental threshold which can be recorded. Smaller events must also occur and must contribute to the total solar radiative output, but they are not recorded due to insufficient resolution of the current instruments.

Our last comment in this subsection is related to nanoflare frequency distribution as a function of its energy. The corresponding function can be formally expressed as follows

$$dN \sim B^{-\alpha} dB \sim W^{-\alpha} dW, \quad \text{for } W \simeq (4 \cdot 10^{20} - 10^{26}) \text{ erg} \quad (3.5)$$

where dN is the number of the nanoflares (including the sub-resolution events) per unit time with energy between W and $W + dW$ which occur as a result of complete annihilation of the anti-nuggets carrying the baryon charges between B and $B + dB$. These two distributions are tightly linked as these two entities are related to the same AQN objects according to (3.4). The energy of the events W in this distribution can be always expressed in terms of the baryon charges B of the AQNs according to (3.3).

The corresponding theoretical estimates of the distribution dN/dB are very hard to carry out as explained in [3]. Fortunately, on the observational (data analysis) side with the estimates dN/dW some progress can be made, and in fact, has been made. In particular, the authors of ref. [30] claim that the best fit to the data is achieved with $\alpha \simeq 2.5$, while numerous attempts to reproduce the data with $\alpha < 2$ were unsuccessful. This is consistent with previous analysis [28] with $\alpha \simeq 2.3$. It should be contrasted with another analysis [32] which suggests that $\alpha \simeq 1.2$ for events below $W \leq 10^{24}$ erg, and $\alpha \simeq 2.5$ for events above $W \geq 10^{24}$ erg. Analysis [32] also suggests that the change of the scaling (the position of the knee) occurs at energies close to $\langle W \rangle \simeq 10^{24}$ erg, which roughly coincides with the maximum of the energy distribution, see Fig.7 in [32].

We conclude this subsection with the following comment. While there is general agreement that the nanoflares (including the sub-resolution events) are responsible for the heating of the corona, there is some disagreement between different groups on spectral properties dN/dW of the flares expressed in terms of power-law index α as defined by (3.5).

3.3 From nanoflares \Rightarrow microflares \Rightarrow large solar flares

The question we want to address in this subsection can be formulated as follows. The nanoflares, as discussed in the previous subsection, can be identified with the AQNs according to (3.4). Furthermore, the nanoflare events (or what is the same the AQN annihilation events) is the main source of the heating corona and as the consequence, the source of the observed EUV radiation (3.2) in agreement with observations (1.1). At the same time, there is a strong argument presented in the Introduction which suggests that the EUV radiation is strongly correlated with large M, X -flares, see Fig. 2 and ref.[2] with details. Therefore, one should expect that these two phenomena (nanoflares versus M,X-flares) characterized by drastically different scales, nevertheless must be originated from the same physics.

The natural question occurs: how it could be ever possible that the M, X -flare events which are characterized by energy scale $W \simeq (10^{26} - 10^{32})$ erg could be related to relatively small objects with energies (3.5) which describe the nanoflares? Such potential relation becomes even more suspicious if one recalls that the nanoflares are distributed very uniformly in quiet regions, as discussed in previous section. It should be contrasted with microflares and large flares which are much more energetic and occur exclusively in active areas.

Our proposed answer on this question will be given at the end of the section. Before we formulate our proposed answer we want to mention that the idea that small nanoflares and large solar flares might be originated from the same physics is not very new, and has been discussed previously in the literature. The basic argument is based on analysis of the flare frequency distribution, similar to (3.5), and is defined as follows

$$dN \sim W^{-\alpha} dW, \quad \text{for } W \simeq (4 \cdot 10^{20} - 10^{32}) \text{ erg}, \quad (3.6)$$

with the only difference in comparison with (3.5) is that the energy W covers entire interesting region. We want to mention two different analysis: ref.[31] which includes RHESSI data with the energies range from 10^{26} erg to 10^{30} erg, and ref. [35] where even super flares with energies 10^{34} erg to 10^{35} erg have been considered.

It has been noted in [31] that it is conceivable that the distribution of all flares follows a single power-law with $\alpha \simeq 2$, which might suggest a common origin for all flares, see Fig. 18 in [31]. Of course, the comparison between different components of the energy distribution is a highly nontrivial procedure as it includes comparison of the data produced by the different instruments with specific instrumental effects. Furthermore, different components of the

energy distribution covers different phases of the solar cycle. Analysis [35] also suggests that all flares (including the superflares) can be described by a single power with $\alpha \simeq 1.8$, see Fig. 18 in [35].

From the AQN dark matter model perspectives the nanoflares and larger flares, beyond the energy window (3.5), are considered to be very different types of events. The nanoflares are identified with AQN according to (3.4) and must be distributed uniformly through the solar surface, which is precisely what has been observed as reviewed in previous subsection. All larger flares distributed very non-uniformly on the solar surface and localized in the active regions (sunspots) which are characterized by a strong magnetic field.

Precisely this distinct feature in spatial distribution constitutes the answer on the question formulated at the beginning of this subsection: the antinuggets (distributed uniformly) play the role of the *triggers* activating the magnetic reconnection of *preexisted* magnetic fluxes in *active regions*. The energy of the flares in this case is generated by the preexisted magnetic field occupying very large area in active region, while relatively small amount of energy associated with initial AQNs play a minor role in the total energy released during a large flare.

We elaborate on this proposal in next section by demonstrating that the AQNs entering the corona from outer space will generate the *shock waves*, playing the role of the triggers, as the velocity of the nuggets $v \sim 10^{-3}c$ is well above the speed of sound, $v/c_{\text{sound}} \gg 1$. The only comment we would like to make here is that this proposal is consistent with the observations that the typical time scale of the nanoflares is (10 – 100) sec. while the large flares last much longer. Furthermore, the typical length scales for these phenomena are also drastically different: the nanoflares are characterized by the scale of order 10^3 km, while a typical characteristic for large flares is around ($10^4 - 10^5$) km. These drastic differences in time and length scales support the idea that AQNs serve as the triggers initiating the larger flares. In this case the time scales of large flares are related to the physics of the magnetic reconnection (measured in hours), in contrast with the annihilation rate of the AQN (measured in seconds), which assumes a typical scale for nanoflares irrespectively to the region where annihilation occurs: whether it is a active or quiet region.

4 AQNs as the triggers initiating the solar flares

We start in subsection 4.1 with a short overview of old Sweet-Parker’s theory on the magnetic reconnection, its development, its results, its problems and difficulties. In subsection 4.2 we present the arguments suggesting that the AQNs entering the solar corona will inevitably generate the shock waves as a result of high velocity of the nuggets $v \sim 10^{-3}c$. One should note that the shock waves will be produced by both kind of species: nuggets and antinuggets. Therefore, in the rest of the paper we do not distinguish different species, in contrast with our discussions of the corona heating proposal [3] reviewed in previous section 3 when the annihilation energy (due to the antinuggets) plays the key role in the arguments.

In the next subsection 4.3 we argue that precisely these shock waves may serve as the triggers which are capable to initiate (ignite) the magnetic reconnections and generate the large flares. Finally, in subsection 4.4 we argue that the observed scaling (3.6) with $\alpha \simeq 2$ can be interpreted in pure geometrical way.

4.1 Magnetic reconnection and Sweet-Parker theory

We start by introducing the most important parameters of the problem

$$S = \frac{Lv_A}{\chi_m}, \quad v_A = \frac{B}{\sqrt{4\pi\rho}}, \quad \chi_m = \frac{c^2}{4\pi\sigma}, \quad (4.1)$$

where S is the so-called the Lundquist number, L is the typical size of the problem, v_A is Alfvén speed, ρ is the plasma’s mass density, χ_m is the magnetic diffusivity, and finally σ is the electrical conductivity of the plasma. The most important parameter for our future estimates is the dimensionless parameter S which assumes the following values for typical coronal conditions, $S \sim (10^{12} - 10^{14})$.

Original idea on magnetic reconnection was formulated by Sweet [36] and Parker [37] sixty years ago. Using simple dimensional arguments, Sweet and Parker (SP) have shown that the reconnection time τ_{rec} is quite slow and expressed in terms of the original parameters of the system as follows

$$\frac{\tau_A}{\tau_{\text{rec}}} \sim \frac{1}{\sqrt{S}}, \quad \tau_A \equiv \frac{L}{v_A}, \quad \frac{u_{\text{in}}}{u_{\text{out}}} \sim \frac{1}{\sqrt{S}}, \quad \frac{l}{L} \sim \frac{1}{\sqrt{S}}, \quad \tau_{\text{rec}} \sim \frac{L}{u_{\text{in}}} \quad (4.2)$$

where u_{in} is the velocity of reconnection between oppositely directed fluxes of thickness l , and $u_{\text{out}} \sim v_A$ is normally assumed to be of order of the Alfvén velocity. The scaling relations (4.2) predicted by SP theory are obviously insufficient to explain the reconnection rates observed in corona due to the very large numerical values of $S \sim (10^{12} - 10^{14})$.

The next step to speed up the reconnection rate has been undertaken in [38] with some important amendments in [39] where it was argued that the reconnection rate could be much faster than the original formula (4.2) suggests. However, some subtleties remained in the proposal [38, 39]. Furthermore, the numerical simulations reproduce conventional scaling formula (4.2) at least for moderately large $S \lesssim 10^4$. In the last 10-15 years large number of new ideas have been pushed forward. It includes, but not limited to such processes as plasmoid- induced reconnection, fractal reconnection, to name just a few.

It is not the goal of the present work to analyze the assumptions, justifications, and the problems related to the old proposals [36–39] and new ideas, and we refer to the recent review papers [35, 40] for recent developments and relevant comments on these matters. The only comment we would like to make here is that the new element (we are advocating in the present work) is the presence of an additional ingredient in the problem which was not a part in the previous studies. This new ingredient of the problem is the AQNs which enter the system from outer space and generate the shock waves in corona as we argue in next subsection 4.2. Our proposal is that precisely these shock waves will serve as the triggers initiating the magnetic reconnections [35–40] which eventually lead to large solar flares.

4.2 AQNs and shock waves in plasma

In this subsection we argue that the AQNs entering the solar corona will inevitably generate the shock waves as a result of high initial velocity of the nuggets $v_{AQN} \sim (10^{-2} - 10^{-3})c$. To simplify the arguments and notations in our presentation below we do not include the magnetic field into consideration at this point². The corresponding generalization with inclusion of a

²Neglecting the magnetic field is sufficiently good approximation in quiet regions when the magnetic energy does not dominate the dynamics. In this case the additional energy is generated exclusively as a result of annihilations of the AQNs with the solar material, while the energy of the magnetic field plays a minor role. The corresponding annihilation events of the AQNs are identified with nanoflares (3.4), and the extra energy due to the annihilation is released as the EUV and x ray radiation as reviewed in section 3.

strong magnetic field (relevant for analysis of the AQNs in the active regions) will be presented in the following section 4.3.

We start our analysis by estimating the speed of sound c_s in corona at $T \simeq 10^6 K$,

$$\left(\frac{c_s}{c}\right)^2 \simeq \frac{3\gamma T}{m_p}, \quad c_s \simeq 7 \cdot 10^{-4} c \cdot \sqrt{\frac{T}{10^6 \text{ K}}}, \quad c_s \simeq 2 \cdot 10^7 \sqrt{\frac{T}{10^6 \text{ K}}} \cdot \left(\frac{\text{cm}}{\text{s}}\right), \quad (4.3)$$

where $\gamma = 5/3$ is a specific heat ratio, and we approximate the mass density ρ of plasma by the proton's number density n as follows $\rho \simeq nm_p$. The crucial observation here is that the Mach number M is always larger than one for a typical dark matter velocities:

$$M \equiv \frac{v_{AQN}}{c_s} \simeq (1.5 - 15) \sqrt{\frac{10^6 \text{ K}}{T}} \gg 1. \quad (4.4)$$

As a result, the shock waves will be inevitably generated when the AQNs enter the solar corona.

In the limit when the thickness of the shock wave can be ignored the corresponding formulae for the discontinuities of the pressure p , temperature T , and the density ρ are well known and given by, see e.g. [41]

$$\begin{aligned} \frac{\rho_2}{\rho_1} &= \frac{(\gamma + 1)M^2}{(\gamma - 1)M^2 + 2}, \\ \frac{p_2}{p_1} &= \frac{2\gamma M^2}{(\gamma + 1)} - \frac{\gamma - 1}{\gamma + 1}, \\ \frac{T_2}{T_1} &= \left(\frac{p_2}{p_1}\right) \cdot \frac{(\gamma + 1)p_1 + (\gamma - 1)p_2}{(\gamma - 1)p_1 + (\gamma + 1)p_2}. \end{aligned} \quad (4.5)$$

For our qualitative analysis which follows we assume that the Mach number $M \gg 1$, in which case the relations (4.5) are greatly simplified and assume the form

$$\frac{\rho_2}{\rho_1} \simeq \frac{(\gamma + 1)}{(\gamma - 1)}, \quad \frac{p_2}{p_1} \simeq M^2 \cdot \frac{2\gamma}{(\gamma + 1)}, \quad \frac{T_2}{T_1} \simeq M^2 \cdot \frac{2\gamma(\gamma - 1)}{(\gamma + 1)^2}. \quad (4.6)$$

The relations (4.6) imply that the discontinuities in temperature T and pressure p could be numerically enormously large as they are proportional to the Mach number M^2 which itself could assume very large number in the given circumstances according to (4.4).

In such a regime (with large Mach numbers $M \gg 1$) the conventional hydro-based computations of the thickness width δ and the absorption coefficient may not be justified and true microscopical computations might be required in this case [41]. Indeed, one can estimate the thermal velocities v_T of the particles in the plasma, kinematic viscosity ν , thickness of the of shock wave δ and the sound absorption coefficient a at $M \gg 1$ to convince yourself that all the relevant parameters are expressed in terms of the mean free path l_0 :

$$v_T \sim \sqrt{\frac{T}{m_p}} \sim c_s, \quad \nu \sim l_0 c_s, \quad a \sim \frac{l_0}{c_s^2}, \quad \delta \sim l_0. \quad (4.7)$$

The estimates (4.7) unambiguously imply that the hydro-based computations cannot be used to study strong shock waves with $M \gg 1$ because the basic assumption that the plasma can be considered as a continuous media (when $l_0 \rightarrow 0$ is assumed to be a smooth limit) cannot be justified.

The mean free path l_0 in corona can be estimated as follows. By definition, $l_0^{-1} \sim \sigma n$, where n is the number density in plasma, and $\sigma \sim \alpha^2/q^2$ is the Coulomb cross section for a typical momentum transfer q . The momentum transfer q can be estimated as a typical impact parameter b in plasma, i.e. $q \sim b^{-1}$, which itself can be expressed in terms of the number density n as follows $b \sim n^{-1/3}$. Collecting all factors together we arrive to the following estimate for l_0 :

$$l_0^{-1} \sim \sigma n \sim \alpha^2 n^{-2/3} n \sim \alpha^2 n^{1/3}, \quad l_0 \sim 10^2 \text{cm} \quad \text{for} \quad n \sim 10^{10} \text{cm}^{-3}. \quad (4.8)$$

Our numerical estimates (4.8) suggest that the thickness width δ of the shock wave can be estimated as follows

$$\delta \sim l_0 \sim 10^2 \text{cm} \cdot \left(\frac{10^{10} \text{cm}^{-3}}{n} \right)^{\frac{1}{3}}, \quad (4.9)$$

which we think is quite reasonable number.

What is the role of the shock waves which will inevitably form when the AQNs enter the solar atmosphere? The total energy due to the annihilation events of the AQNs (identified with nanoflares according to (3.4)) is fixed and determined by the dark matter density according to the estimate (3.2) which agrees with observations (1.1). As we discussed in [3] and reviewed in section 3 this energy is sufficient to heat the corona to $T \simeq 10^6 \text{K}$. There are many mechanisms which are capable to transfer energy from AQNs to plasma. The shock waves and the turbulent boundary layer which always accompanies a body moving with $M > 1$ eventually must play a key role in this energy transfer from AQNs (nanoflares) to the plasma³.

Apparently, a structure which resembles very much a jet (which is a typical shape of a shock wave) has been observed in the chromosphere [42], see also review [35]. We'll discuss the observational consequences of our proposal in more details in subsection 5. Now we want to make a short comment that the observed jets, coined as "chromosphere anemone jets" in [42] are few thousand kilometres long and few hundred kilometres wide. Such a cone-like shape indeed represents a typical morphology for a body moving with $M > 1$ which generates a shock wave. The observed tiny jets are also characterized by a typical for nanoflares energy (3.5) which can be interpreted as an additional indirect support of our identification (3.4) of AQNs generating the shock waves with nanoflares conjectured long ago [24].

4.3 Magnetic reconnection ignited by the shock waves

The question we address in this section can be formulated as follows: what happens if the AQNs generating the shock waves with $M \gg 1$ as discussed above, will enter the active region with sufficiently large magnetic field? In this case the dynamics of the magnetic field cannot be ignored and must be included into the consideration. There are few important parameters which control the dynamics of the system: in addition to already defined parameters (4.1) it is convenient to introduce another dimensionless parameter β which determines the importance of the magnetic pressure,

$$\beta \equiv \frac{8\pi p}{B^2} \sim 0.5 \cdot 10^{-1} \left(\frac{n}{10^{10} \text{cm}^{-3}} \right) \cdot \left(\frac{T}{10^6 \text{K}} \right) \cdot \left(\frac{100 \text{G}}{B} \right)^2, \quad (4.10)$$

³The corresponding hard questions on energy transfer are well beyond the scope of the present work. The only comment we would like to make here is that the corresponding estimates are likely to require a truly microscopical computations as mentioned above.

where for numerical estimates we use typical parameters for the active regions in corona when $\beta \ll 1$. Another important parameter is Alfvén speed v_A which assumes the following numerical value in this environment

$$\frac{v_A}{c} = \frac{B}{c\sqrt{4\pi\rho}} \sim \left(\frac{B}{100 G}\right) \cdot \sqrt{\frac{10^{10} \text{ cm}^{-3}}{n}} \sim 0.2 \cdot 10^{-2}, \quad v_A \simeq 6 \cdot 10^7 \frac{\text{cm}}{\text{s}}. \quad (4.11)$$

For these parameters the numerical value for v_A is the same order of magnitude as the speed of sound c_s according to (4.3). This remark will play an important role in our arguments which follow.

With these preliminary comments we are in position to formulate the key question of this section: what happens when the AQN enters the region with $\beta \ll 1$ and generates the shock wave with $M \gg 1$ as described in section 4.2? The proposed answer is that the extra pressure (4.6) due to the shock wave will compress the region where the magnetic fields have opposite directions and where the magnetic reconnection starts. Precisely this is the region where the current sheet is generated, which eventually transforms the energy of the magnetic field into the radiation.

Before we continue with our numerical estimates we must say that the idea that the shock waves may drastically increase the rate of magnetic reconnection is not new, and have been discussed previously in the literature [43], though in quite different context: it was applied to interstellar medium in the presence of the supernova shock. The new element which is advocated in the present work is that the small shock waves resulting from entering the AQNs are widespread and generic events in solar corona within AQN dark matter scenario. As a result of this generality the flares (which are generated as a result of the magnetic reconnections) must be also very typical and ubiquitous events which must be correlated with dark matter flux. This is precisely the correlations which have been analyzed in [2], and which was the main motivation for the present studies.

The key element in our arguments suggesting that the shock wave may drastically modify the rate of magnetic reconnection is based on observation that the pressure and the temperature experience some dramatic changes when the shock wave approaches the reconnection region. To be more precise the extra term Δp due to the large Mach number (4.6) must be added to the total pressure during the short period of time of passage of the shock wave through the (future) reconnection region

$$\Delta p \equiv (p_2 - p_1), \quad \frac{\Delta p}{p_1} \simeq M^2 \cdot \frac{2\gamma}{(\gamma + 1)} \gg 1, \quad (4.12)$$

where subscript p_1 corresponds to the unperturbed system without shock wave. The main observation here is that the extra pressure strongly affects (locally) the parameter β ,

$$\Delta\beta \equiv \frac{8\pi\Delta p}{B^2} \sim 0.5 \cdot 10^{-1} \cdot \left(\frac{2\gamma M^2}{\gamma + 1}\right) \cdot \left(\frac{n}{10^{10} \text{ cm}^{-3}}\right) \cdot \left(\frac{T}{10^6 K}\right) \cdot \left(\frac{100 G}{B}\right)^2. \quad (4.13)$$

Similar modifications also occur for the density $\Delta\rho$ and the temperature ΔT according to eqs. (4.6). The crucial observation here is that the effective parameter $\Delta\beta$ given by (4.13) can become numerically very large in contrast with unperturbed case (4.10) when this parameter is typically very small. Indeed, for $M^2 \gtrsim 10$ which can be easily achieved according to estimate (4.4), the parameter $\Delta\beta > 1$ becomes larger than one. In fact it could become enormously large. The great numerical value for this dimensionless parameter unambiguously suggests

that the magnetic flux can be easily pushed into the direction to the current sheet region where the reconnection starts. Precisely this scenario (when $\Delta T/T \gg 1$ and $\Delta p/p \gg 1$ in spatially very small region for a very short period of time) represents a proposed mechanism for the reconnection triggered and initiated by the shock wave with large Mach number M , which itself is an inevitable consequence of the dark matter AQNs entering the solar atmosphere.

Now we want to estimate the size and the energy scales associated with such events. We consider separately two different stages. First, we estimate the scales related to the initial phase of the evolution when the AQNs produce the shock waves, but the magnetic reconnection has not started yet. The estimation for the second phase assumes that the magnetic reconnection, leading to a large solar flare, is already fully developed.

In the first, initial stage of the evolution, the magnetic reconnection has not started yet, and entire energy is related to the shock wave, which itself forms as a result of AQN entering the solar atmosphere from outer space. In this case a typical time scale when AQN completely annihilates its baryon charge is similar to estimation [3] for the nanoflares and is of order of $\tau \sim (10 - 10^2)$ sec. A typical length scale is determined by the initial velocity of the AQN which is of order $v_{\text{AQN}} \sim 10^{-3}c$ such that $L \sim v_{\text{AQN}} \cdot \tau \sim (10^3 - 10^4)$ km. At the same time, a typical radius R of the cone formed by the shock wave is determined by the speed of sound c_s , such that $R \sim M^{-1}L$, where Mach number M is estimated in (4.4). For numerical estimates below we take $M \simeq 10$. The affected volume of the cone due to the shock wave is estimated as $V \simeq (\pi R^2 L)/3 \sim 10^{-2}L^3$. We summarize the parameters of the initial stage as follows

$$\tau \sim (10 - 10^2) \text{ sec}, \quad L \sim (10^3 - 10^4) \text{ km}, \quad R \sim 10^{-1}L, \quad V \sim \frac{\pi R^2 L}{3} \sim 10^{-2}L^3. \quad (4.14)$$

We are now in position to estimate the typical energetic characteristics of the system during this initial stage. The key element is the observation that the temperature T experiences a large discontinuity resulting from the shock according to (4.6). Therefore, we estimate a typical temperature as follows

$$\frac{T_2}{T_1} \simeq M^2 \cdot \frac{2\gamma(\gamma - 1)}{(\gamma + 1)^2} \sim 10^2, \quad \Delta T \equiv (T_2 - T_1) \sim M^2 T_1 \sim 10^8 \text{ K} \quad (4.15)$$

where $T_1 \sim 10^6 \text{ K}$ corresponds to unperturbed temperature before the shock passage through the area. Important comment here is that formula (4.15) shows that there is a finite portion of the volume V_{shock} where temperature is very high $T \sim 10^8 \text{ K}$. These regions with high temperature could be the source of the 10 keV x-rays which are normally observed few moments before the flare starts. We elaborate on this point in next section 5 devoted to the observational evidences of this proposed mechanism treating AQNs as the triggers of the flares.

The second, fully developed stage of the flare in this framework is due to the magnetic reconnection ignited by the shock wave as described above. We have nothing new to say about this conventional phase of the evolution. We present the corresponding formula for the total flare's energy for completeness and future estimates,

$$E_{\text{flare}} \sim \frac{B^2}{8\pi} \cdot V_{\text{flare}} \sim 0.3 \cdot 10^{31} \text{ erg} \left(\frac{B}{300 \text{ G}} \right)^2 \cdot \left(\frac{V_{\text{flare}}}{10^{13} \text{ km}^3} \right), \quad V_{\text{flare}} = L_{\perp}^2 L_z, \quad (4.16)$$

where $L_z \sim 5000 \text{ km}$ is a typical height of the solar corona where the magnetic field is large, while L_{\perp}^2 is the area in active region (sunspots) which eventually becomes a part of magnetic

reconnection producing the large flares. It is assumed that precisely this region of volume $V_{\text{flare}} = L_{\perp}^2 L_z$ with large average magnetic field B feeds the solar flare as a result of magnetic reconnection.

It is quite obvious that the energy (4.16) of a fully developed flare is many orders of magnitude larger than the initial energy related to the shock wave which serves as a trigger of a large flare. Nevertheless, this initial stage in the flare evolution plays a key role in future development of the system because it provides a very strong impulse with $\Delta T/T \gg 1$ and $\Delta p/p \gg 1$ in very small and very localized area for very short period of time (4.14) in the region where the magnetic reconnection eventually develops.

4.4 Geometrical interpretation of the scaling $dN \sim W^{-\alpha} dW$

In this subsection we would like to interpret the observed scaling (3.6) for the frequency of appearance of large flares in geometrical terms within scenario advocated in this work. For this purpose it is more convenient to integrate formula (3.6) over energy dW to represent it in the following form

$$N(W) \simeq C \left(\frac{W_0}{W} \right) \quad \text{for} \quad \alpha \simeq 2 \quad \text{and} \quad W \simeq (10^{26} - 10^{32}) \text{ erg}, \quad (4.17)$$

where we include energy window for microflares and flares with their typical energies. We also assume $\alpha \simeq 2$ as advocated in [31], see also review [35]. The coefficient C is the normalization factor which has dimensionality $(\text{year})^{-1}$ with $W_0 \simeq 10^{26}$ erg as a part of this normalization's convention. In these notations the $N(W)$ represents the number of flare events per year with energy of order W . In formula (4.17) we excluded the nanoflare events from our present analysis because this section is devoted to studies of large flares in active regions while nanoflares have been mostly discussed in relation with physics of EUV radiation in quiet regions, see section 3.2 for review. Our goal here is to argue that the observed W^{-1} scaling in eq.(4.17) can be interpreted in terms of geometrical parameters of the active regions within our framework.

We start our analysis with few preliminary comments. A shock wave (initiated by the AQN) will successfully ignite a large flare if it passes through the region where future magnetic reconnection may occur, i.e. the area, where magnetic fluxes have opposite directions and are sufficiently close to each other. From eq. (4.2) one can infer that a typical distance l between preexisted oppositely directed fluxes is of order $l \sim L/\sqrt{S} \sim 10$ m for $S \sim 10^{12}$ and $L \sim 10^4$ km. Our comment here is that the shock front must pass through this region $\sim l$ to ignite the large flare. If the shock waves characterized by parameters (4.14) do not overlap with this region of pre-existed fluxes than the corresponding annihilation events will manifest themselves as the conventional nanoflare type events with sub resolution energies reviewed in Section 3.2. However, if the same AQNs pass through a small reconnection area $\sim l$ than a large flare may be ignited as will be explained below.

One can estimate the corresponding probability of ignition of a large flare as follows. The total number of AQNs entering the solar atmosphere per unit time can be estimated from (3.2) as follows

$$N_{\odot(\text{AQN})} \sim \frac{L_{\odot(\text{AQN})}}{\langle B \rangle} \sim 10^5 \left(\frac{10^{25}}{\langle B \rangle} \right) \frac{1}{\text{s}} \sim 10^{12} \left(\frac{10^{25}}{\langle B \rangle} \right) \frac{1}{\text{year}}, \quad (4.18)$$

which is consistent with the estimates [26, 28] on total number of nanoflares (including the sub resolution events) over the whole Sun, see also related comments in [3]. The probability

that the AQNs fall into the active regions is roughly proportional to the total yearly averaged sunspot area. The corresponding sunspot area strongly depends on the solar cycle but on average can be estimated as $\sim 10^4 \mu\text{Hem}$, see e.g. [44]. Therefore, the corresponding suppression factor can be estimated as $\sim 10^{-2}$.

Another important suppression factor $(R/L_{\perp})^2$ is related to the smallness of the shock wave cone size R^2 in comparison with much larger sunspot area L_{\perp}^2 as explained above. It is important to emphasize that the same sunspot area L_{\perp}^2 also enters the expression for the volume $V_{\text{flare}} = (L_{\perp}^2 L_z)$ in eq. (4.16) which describes the magnetic energy potentially available for its transferring into the flare heating as a result of magnetic reconnection. We assume in what follows that a typical averaged magnetic field B over the entire regions in the active area, the relevant height L_z of the solar atmosphere effectively contributing to the total energy of the flare (4.16) and the shock wave cone size R^2 assume (approximately) the same typical values as these parameters should be treated as the external parameters with respect to the magnetic reconnection dynamics. With the assumption just formulated we infer that the energy of the flare scales according to (4.16) as $E_{\text{flare}} \sim L_{\perp}^2$, while the probability to ignite the magnetic reconnection in area L_{\perp}^2 is proportional to $(R/L_{\perp})^2 \sim E_{\text{flare}}^{-1}$ as discussed above. Therefore, the observed relation (4.17) in our framework has a geometrical interpretation, as the frequency N of appearance of a flare with energy of order E_{flare} scales as $N \sim L_{\perp}^{-2} \sim E_{\text{flare}}^{-1}$.

Having determined the scaling features of the flares we are now in position to estimate the normalization coefficient C which enters the formula (4.17). There are three suppression factors contributing to $C \equiv C_1 C_2 C_3$. The first two suppression factors have been already mentioned: it includes the smallness of the sunspot areas (suppression $C_1 \sim 10^{-2}$) and the smallness of the region which shock wave is capable to sweep being already inside the active sunspot area. The corresponding suppression can be estimated numerically as $C_2 \sim R^2/L_{\perp}^2 \sim (10^{-4} - 10^{-2})$ depending on the specific features of a sunspot region. There is one more suppression factor C_3 which accounts for ‘‘preparedness’’ of magnetic field configuration when the reconnection is ready to start if the shock wave sweeps the ‘‘would be’’ reconnection region.

We proceed with the corresponding estimate C_3 by comparing the observable frequency of appearance of the flares, see e.g. Fig.18 in [31] with formula (4.17). In particular, with our normalization for $E_{\text{flare}} \sim 10^{26} \text{erg}$ one concludes that $C \sim 10^4$ flares/year. One arrives to a similar result if one uses a different energy (e.g. $E_{\text{flare}} \sim 10^{29} \text{erg}$) for the normalization because the scaling $N \sim E_{\text{flare}}^{-1}$ is shown to be consistent with the observations. Comparing this estimate with our previous estimates for C_1 and C_2 and with total number $N_{\odot(\text{AQN})}$ of AQNs entering the solar corona per unit time (4.18) one concludes that $C_3 \simeq (10^{-1} - 10^{-3})$. The corresponding suppression factor can be attributed to the level of preparedness of magnetic field configuration for the magnetic reconnection to be successful. In other words, this suppression factor describes the probability that there is at least one a ‘‘would be’’ reconnection area in the active region where the magnetic configuration is already built in and prepared to explode⁴ if the shock wave passes through this area and triggers the flare.

We conclude this subsection with the following comment. There are many factors which might be responsible for a slight deviation of the observed scaling with $\alpha \simeq 1.8$ as fitted in ref. [35] and simple formula (4.17) with $\alpha = 2$ which permits a pure geometrical interpretation as explained above. The corresponding analysis is well beyond the scope of the present work as

⁴In other words, the magnetic fluxes are oppositely directed with a large gradient and properly located being sufficiently close to each other on a distance of order $\sim l$.

the main goal here is to present a big picture rather than to analyze some minor details to this proposal.

As we already mentioned, our original contribution to this field is entirely related to the initial stage of the evolution summarized by parameters (4.14), (4.15). We also argued that this proposal is consistent with the observed scaling (4.17). Furthermore, this proposal (when the AQNs play the role of the triggers) naturally resolves the problem of drastic separation of scales when a flare itself lasts for about an hour while the preparation phase of the magnetic configurations to be reconnected (coded by coefficient C_3 discussed above) could last for months. These two drastically different scales can peacefully coexist in our framework because the presence of a trigger in the system which is not an internal part of the magnetic reconnection's dynamics.

Explicit numerical simulations supporting the estimates presented above in any realistic environment are well beyond the scope of the present work due to large number of technical and conceptual problems which need to be understood⁵. Rather, we present in next section 5 some observational evidences supporting this specific mechanism and entire framework in general. It is interesting to note that a 2d MHD simulations [43] developed for very different environment with very different purposes in very different context nevertheless show that the shock waves indeed may trigger and ignite sufficiently fast reconnections⁶.

5 AQNs as triggers of solar flares: proposal confronting the observations

In this section we want to list a number of observations which apparently show that the suggested mechanism when a large flare is triggered by a small scale jet-like structure due to the shock wave (identified according to (3.4) with AQN/nanoflare) is consistent with those observations.

5.1 Pre-flare x-ray radiation: intensity, timing and direction of the flare propagation (from top to bottom)

In this subsection we choose a specific studies [45] of the X-ray analysis of the X6.9 flare on August 9.2011 in order to be more specific in our arguments which follow. We assume that the observed features are generic properties of solar flares. We want to emphasize on three important elements of the analysis relevant for our studies and related to the initial stage of the evolution, which is commonly referred to as a pre-flare phase:

1. It has been observed in [45] that the x-rays in (0.1–0.8)nm frequency bands experience very sharp (almost vertical) enhancement with a typical scale of variation measured in seconds. This frequency band corresponds to (1.2 – 10) keV x-rays. At the same time, the 9.4 nm line corresponding to 1 keV energy shows a less profound, but still noticeable, enhancement with a

⁵In particular, as we already mention, when the Mach number M becomes very large, the conventional hydro-based computations may not be justified as all relevant parameters (4.7) are expressed in terms of the mean free path l_0 which obviously inconsistent with conventional treatment of a continuum media when the limit $l_0 \rightarrow 0$ is supposed to be smooth. Another problem with the modelling of this scenario is that the turbulent boundary layer which always accompanies a fast moving body should play a key role in the energy exchange of the AQNs with the solar material. This rate of the energy exchange (which is hard to compute) obviously should play an important role in any estimates of the dynamics of magnetic reconnection.

⁶Furthermore, the 2d MHD simulations [43] show that a large number of different phenomena, including SP reconnection [36, 37], Petschek reconnection [38, 39], tearing instability, formation of the magnetic islands, and many others, may all take place at different phases in the evolution of the system, see also reviews [35, 40].

typical scale of variation measured in few minutes. Low-energetic 33.5 nm line demonstrates even smaller variation;

2. The enhancement of the (1.2 – 10) keV band is enormous and could be as large as 2-3 orders of magnitude in comparison with its background values, see Fig.8 in [45];

3. It has been observed in [45] that “the pre-flare enhancement propagates from the higher levels of the corona into the lower corona and chromosphere.” This claim has been inferred from analysis of intensities of different lines during the pre-flare.

In our proposal all these features are direct consequences of the basic picture and very naturally occur. Indeed, the high temperature $T \simeq 10^8\text{K}$ in the region where the shock wave propagates is related to the large Mach number as equation (4.15) states. Therefore, it is not a surprise that the hard x-rays with energy ~ 10 keV can be easily radiated from this region. Furthermore, the very sharp enhancement during very short period of time is also perfectly consistent with our estimates (4.14) which suggests that precisely this time scale of $(10 - 10^2)$ sec determines the typical timing of the cone produced by the shock wave. Finally, the propagation of the flare in the direction from top atmosphere to its bottom, as mentioned in item 3 above, is perfectly consistent with our proposal as the dark matter AQNs which generate the shock waves enter the solar atmosphere from outer space. Therefore, they first enter the higher levels of the corona where they generate the shock wave, before they reach chromosphere in $\tau \sim (10 - 10^2)$ sec.

5.2 Shapes of the anemone jets

It has been known for quite sometime that the morphology for large scale flares and small scale flares (nanoflares, microflares) are drastically different. To be more specific: the large scale flares are bubble like or flux rope type, while the small scale flares (nanoflares, microflares) are jets or jet-like, see e.g. review [35].

This qualitative difference in the morphology can be easily understood in our framework, where the nanoflares (directly identified with AQNs according to (3.4)) are always jet like as they inevitably generate the shock waves as discussed in Section 4. At the same time, if the AQNs enter the active regions with large magnetic field, these shock waves serve as the triggers for the larger flares. In this case the original morphological shape (jet-like structure) characterized by the scales (4.14) is completely washed out by a much larger scale phenomena, the magnetic reconnection, leading to larger flares characterized by drastically different sizes, shapes, and the energy scales (4.16).

We want to mention in this subsection ref. [42] devoted to analysis of the anemone jets *outside* of sunspots of active regions. It has been claimed in [42] that the observations show the “ubiquitous presence of chromospheric anemone jets outside of sunspots...”. The typical characteristics are:

$$L \sim (2000 - 5000) \text{ km long}, \quad R \sim (150 - 300) \text{ km wide}, \quad (5.1)$$

which are perfectly consistent with our estimates (4.14) based on the picture where the ratio $L/R \sim 10$ is large as a result of the development of the shock wave with large Mach number $M \sim 10$ according to (4.4).

The results of [42] are consistent with our proposal [3] that AQNs (identified with nanoflares (3.4)) in *quiet* regions represent very generic events which are capable to heat corona and chromosphere as reviewed in Section 3. If these AQNs are sufficiently small and belong to a sub-resolution domain, they cannot be directly observed as discussed in Section 3.2, but they must be present in the system to heat the corona. The larger AQNs can produce

larger shock waves (4.14) which can be measured and are compatible with observations (5.1) from quiet regions.

5.3 Other related phenomena: sunquakes

We also want to mention some other observations which might be also related to the shock waves which are inevitably generated as a result of the dark matter AQNs entering the solar atmosphere from outer space. We want to make few comments on possible relation with sunquakes (acoustic pulses propagating below the visible surface) which have been observed and analyzed in details, see e.g. recent papers [46, 47]. However, the nature of the sunquakes remains unknown due to a number of very puzzling features which can be highlighted as follows.

It has been known for quite sometime that the sunquake events are well correlated with hard x-ray emission (during the impulsive phase) of the flare. The conventional wisdom is that the flare energy is released in the corona and drives an acoustic disturbance in the solar interior, very close to the photospheric layer. For this mechanism to be operational one should assume that the energy must propagate through nine pressure scale heights. There are many estimates demonstrating that such energy transfer is almost impossible. At least, it is very hard to imagine how it could happen within conventional astrophysical processes [46, 47]. The picture becomes even more puzzling because the acoustic enhancements occur only in certain locations within the flaring active region. Furthermore, the acoustic enhancements are not detected for every flare. Authors of ref. [47] suggested that a single, large temperature increase might explain some of the observations. However, no any hints (what might be the cause for such an instantaneous large temperature increase) were given in [47]. Authors of ref. [46] suggested that "the energy is transported downwards in a fashion that is somehow *invisible* to our observations".

Our original comment here is that while the energy transport due to the conventional physical processes is indeed unlikely to occur, the AQNs which play the role of the triggers of the flares as argued in the present work, may easily propagate and penetrate to very deep regions of the solar photosphere. After that they can serve as the triggers to ignite the sunquakes. Essentially, we propose that the nuggets play the same role in photosphere as they play in upper atmosphere by initiating the flares as described in this work.

The main idea behind of this proposal is that a nugget ignites the flare in the upper atmosphere and continues to move to photosphere without losing much velocity and momentum as a result of its very small size and very high velocity as reviewed in section 2. Because the speed of sound at the latitude ~ 100 km could be an order of magnitude smaller than at higher altitudes (4.3), the nugget may ignite a new shock wave in addition to the previous shock wave in upper corona where it triggered the flare as discussed in section 4. In other words, formulae (4.4) and (4.6) in photosphere assume the form

$$M_{\text{photosphere}} \equiv \frac{v_{\text{AQN}}}{c_s} \simeq (1.5 - 15) \sqrt{\frac{10^4 \text{ K}}{T}} \gg 1, \quad v_{\text{AQN}} \sim 10^{-4}c \quad (5.2)$$

$$\frac{p_2}{p_1} \simeq M_{\text{photosphere}}^2 \cdot \frac{2\gamma}{(\gamma + 1)}, \quad \frac{T_2}{T_1} \simeq M_{\text{photosphere}}^2 \cdot \frac{2\gamma(\gamma - 1)}{(\gamma + 1)^2},$$

such that very strong shock wave with $M_{\text{photosphere}} \gg 1$ may trigger the sunquake precisely in the specific location where AQN enters a relatively dense region of the photosphere. This is because the shock wave generated due to the large Mach number may produce a single

highly localized increase of the temperature $\Delta T/T \gg 1$ and pressure $\Delta p/p \gg 1$ deep in the atmosphere.

In this case the observed correlations between the flares and the sunquakes is a direct consequence of the fact that both events are ignited by the same quark nugget which moves with velocity $v_{\text{AQN}} \sim 10^{-4}c$ when the nuggets reach the photosphere. Furthermore, the observation that the acoustic enhancements occur only in certain locations within the flaring active region is also easy to understand: it is not the large flare itself which feeds the sunquake. Rather the quake is localized in the area where the nugget enters the photosphere and ignites a local disturbance leading to the sunquake. The observed larger Doppler velocity shifts in comparison with locations with no sunquake is also easy to interpret and similar to the Doppler shifts discussed for nanoflares as reviewed in Section 3.2 after eq. (3.4).

If we accept this proposal, one may wonder why the acoustic enhancements are not generated for every flare. The answer might be related to the fact that in that cases the largest portion of the AQN got annihilated on its way from corona to photosphere, in which case a sufficiently energetic shock wave could not be formed to play the role of a trigger for the acoustic disturbance. In other words, only sufficiently large and fast nuggets are capable to reach the photosphere.

6 Conclusion and final remarks

The main claim of the present work is that the nanoflares conjectured by Parker long ago to resolve the corona heating problem, may also trigger the larger solar flares. In our framework the nanoflares are identified with AQNs according to (3.4). In the previous paper [3] we argued that the nanoflares may explain the EUV radiation from corona as a result of the annihilation processes of the AQNs with the solar material according to estimate (3.2) which is perfectly consistent with observations (1.1). In the present work we argue that exactly the same nuggets entering the regions with high magnetic field may ignite the magnetic reconnections which eventually lead to much larger flares. This proposal explains unexpected and bizarre correlations observed in [2] between EUV intensity, frequency of flares and positions of the planets as a result of the gravitational lensing of "invisible" streaming matter towards the Sun. We identify the "invisible" streaming matter from [2] with AQNs studied in [3] and in present work. Furthermore, we also argued that the sunquakes may also be triggered by the same AQNs when they reach the photospheric layer.

Technically, the magnetic reconnection which feeds the flare is ignited due to the shock wave which inevitably develops when the AQN enters the solar atmosphere with velocity $v_{\text{AQN}} \sim 10^{-3}c$ which is much greater than the speed of sound in the corona. The corresponding large value of the Mach number $M = v_{\text{AQN}}/c_s \gg 1$ unambiguously implies that the shock waves will be formed and may initiate the flares due to the very strong and very short impulses expressed in terms of pressure $\Delta p/p \sim M^2$ and temperature $\Delta T/T \sim M^2$ if occur in vicinity of (would be) magnetic reconnections area in active regions.

We also argued that this picture is consistent with observations on intensity of the x-ray radiation in pre-flare phase and studies of the anemone jets. It may also explain the nature of the sunquakes as discussed in section 5. It is also consistent with observed scaling for frequency of appearance of a flare with a given energy as argued in section 4.4. This proposal (when AQN plays role of a trigger) also resolves a problem of drastic separation of scales when a flare itself lasts for an hour while the preparation phase of the magnetic configurations (to be reconnected) could last for months.

We conclude this work with following proposals for the futures studies which may further support (or rule out) this mechanism.

- First of all, a similar EUV and x-ray radiation correlated with the flares as discussed in the present work (and observed in the Sun, see Fig.2) must be present in many similar stars, though the intensity and the spectral properties are highly sensitive to the specific features of stars and their positions in the galaxy. The intensity and spectral properties of the radiation must obviously depend on the outer dark matter density $\rho_{\text{DM}}(r)$ which itself strongly depends on position of the star with respect to the galactic center.
- Secondly, our conjecture that sunquakes are related to the same AQNs which ignite the flares can be tested by studies of the cross-correlations similar to analysis advocated in [2] (see Fig. 1 as a sample) when instead of “number of flares” one should study the “number of sunquakes” along the “y” axis.
- Thirdly, our arguments that the large flares are ignited by the AQNs when they enter the active regions with strong magnetic field can be tested by analyzing of the cross-correlations similar to studies advocated in [2] when instead of “number of flares” one should study the “number of sunspots” (or total area of the sunspots) along the “y” axis as a function of the heliocentric longitude of the planets along “x” axis.

Acknowledgements

I am thankful to Konstantin Zioutas for explaining their paper [2] which motivated the present studies. I am also thankful to Kyle Lawson and Ludovic Van Waerbeke for discussions and comments. This research was supported in part by the Natural Sciences and Engineering Research Council of Canada.

References

- [1] J. A. Klimchuk, *Solar Phys.* **234**, 41 (2006) [astro-ph/0511841].
- [2] S. Bertolucci, K.Zioutas, S. Hofmann, M. Maroudas, *Physics of the Dark Universe* (2017), doi.org/10.1016/j.dark.2017.06.001, [arXiv:1602.03666 [astro-ph.CO]]
- [3] A. Zhitnitsky, *JCAP* **1710**, no. 10, 050 (2017) doi.org/10.1088/1475-7516/2017/10/050 [arXiv:1707.03400 [astro-ph.SR]].
- [4] A. R. Zhitnitsky, *JCAP* **0310**, 010 (2003) [hep-ph/0202161].
- [5] K. Lawson and A. R. Zhitnitsky, *Snowmass 2013 e-Proceedings*, arXiv:1305.6318 [astro-ph.CO].
- [6] X. Liang and A. Zhitnitsky, *Phys. Rev. D* **94**, 083502 (2016) [arXiv:1606.00435 [hep-ph]].
- [7] S. Ge, X. Liang and A. Zhitnitsky, *Phys. Rev. D* **96**, no. 6, 063514 (2017) [arXiv:1702.04354 [hep-ph]].
- [8] R. D. Peccei and H. R. Quinn, *Phys. Rev. D* **16**, 1791 (1977);
S. Weinberg, *Phys. Rev. Lett.* **40**, 223 (1978);
F. Wilczek, *Phys. Rev. Lett.* **40**, 279 (1978).
- [9] J.E. Kim, *Phys. Rev. Lett.* **43** (1979) 103;
M.A. Shifman, A.I. Vainshtein, and V.I. Zakharov, *Nucl. Phys.* **B166** (1980) 493(KSVZ-axion).
- [10] M. Dine, W. Fischler, and M. Srednicki, *Phys. Lett.* **B104** (1981) 199;
A.R. Zhitnitsky, *Yad.Fiz.* **31** (1980) 497; *Sov. J. Nucl. Phys.* **31** (1980) 260 (DFSZ-axion).
- [11] K. van Bibber and L. J. Rosenberg, *Phys. Today* **59N8**, 30 (2006);

- [12] S. J. Asztalos, L. J. Rosenberg, K. van Bibber, P. Sikivie, K. Zioutas, *Ann. Rev. Nucl. Part. Sci.* **56**, 293-326 (2006).
- [13] Pierre Sikivie, *Lect. Notes Phys.* **741**, 19 (2008) arXiv:0610440v2 [astro-ph].
- [14] G. G. Raffelt, *Lect. Notes Phys.* **741**, 51 (2008) [hep-ph/0611350].
- [15] P. Sikivie, *Int. J. Mod. Phys. A* **25**, 554 (2010) [arXiv:0909.0949 [hep-ph]].
- [16] L. J. Rosenberg, *Proc. Nat. Acad. Sci.* (2015),
- [17] P. W. Graham, I. G. Irastorza, S. K. Lamoreaux, A. Lindner and K. A. van Bibber, *Ann. Rev. Nucl. Part. Sci.* **65**, 485 (2015) [arXiv:1602.00039 [hep-ex]].
- [18] A. Ringwald, *PoS NOW* **2016**, 081 (2016) [arXiv:1612.08933 [hep-ph]].
- [19] D. M. Jacobs, G. D. Starkman and B. W. Lynn, *Mon. Not. Roy. Astron. Soc.* **450**, no. 4, 3418 (2015) [arXiv:1410.2236 [astro-ph.CO]].
- [20] S. Ge, X. Liang and A. Zhitnitsky, arXiv:1711.06271 [hep-ph].
- [21] A. Zhitnitsky, *Phys. Rev. D* **74**, 043515 (2006) [astro-ph/0603064].
- [22] D. H. Oaknin and A. R. Zhitnitsky, *Phys. Rev. Lett.* **94**, 101301 (2005), [arXiv:hep-ph/0406146].
- [23] A. Zhitnitsky, *Phys. Rev. D* **76**, 103518 (2007) [astro-ph/0607361].
- [24] E.N. Parker, *ApJ*, **264**, 642 (1983); *ibid.* **330**, 474 (1988).
- [25] S. Krucker, A. O. Benz, *Solar Phys.* **191**, 341, (2000).
- [26] S. Krucker, A. O. Benz, *ASP Conference Series*, Vol. **200**, (2001) P. Brekke, B. Fleck, and J. B. Gurman eds, [arXiv:astro-ph/0012106].
- [27] U. Mitra Kraev, A. O. Benz, *A&A*, **373**, 318, (2001).
- [28] A. O. Benz, S. Krucker, *Astrophys. J.*, **568**, 413, (2002).
- [29] A. O. Benz, P. Grigis, *Advances in Space research*, **32**, 1035 (2003) [arXiv:astro-ph/0308323].
- [30] A. Pauluhn and S. K. Solanki, *Astron. Astrophys.* **462**, 311 (2007) [astro-ph/0612585].
- [31] I. G. Hannah, S. Christe, S. Krucker, G. J. Hurford, H. S. Hudson and R. P. Lin, *Astrophys. J.* **677**, 704 (2008) [arXiv:0712.2544 [astro-ph]].
- [32] S. Bingert and H. Peter, *Astron. Astrophys.* **550**, A30 (2013) [arXiv:1211.6417 [astro-ph.SR]].
- [33] Terzo, S., Reale, F., Miceli, M., et al., *Astrophys. J.*, **736**, 111 (2011);
Bradshaw, S. J., Klimchuk, J. A., and Reep, J. W., *Astrophys. J.*, **758**, 53 (2012);
D. B. Jess, M. Mathioudakis, P. H. Keys, *Astrophys. J.*, **795**, 172, (2014).
A. S. Kirichenko and S. A. Bogachev, *Astrophys. J.*, **840**, 45, (2017);
Cecilia Mac Cormack et al, *Astrophys. J.*, **843**, 70, (2017).
- [34] J. A. Klimchuk and Hinode Review Team, "Achievements of Hinode in the First Ten Years," 2017, PASJ, submitted [astro-ph/1709.07320].
- [35] Kazunari Shibata and Shinsuke Takasao, "Fractal Reconnection in Solar and Stellar Environment", arxiv:1606.09401
- [36] P. A. Sweet, *IAU Symposium vol* **6**, 123 (1958)
- [37] E. N. Parker, *J. Geophys. Res.* **62** 509 (1957)
- [38] H. E. Petschek, *NASA Special Publication* **50** 425 (1964)
- [39] R. M. Kulsrud, *Earth Planets Space* **53** 417 (2001)
- [40] N.F.Loureiro and D. A. Uzdensky, *Plasma Phys. Control Fusion* **58** 014021 (2016), arxiv: 1507.07775

- [41] L.D.Landau and E.M. Lifshitz, Fluid Mechanics, Butterworth-Heinemann, 2nd edition, 1987.
- [42] K. Shibata, T. Nakamura, T. Matsumoto, et al.: Chromospheric Anemone Jets as Evidence of Ubiquitous Reconnection. *Science*, **318** 1591 (2007), arxiv: 0810.3974
- [43] S.Tanuma, T. Yokoyama, T. Kudoh, and K. Shibata *ApJ*, **551**, 312 (2001)
- [44] S. Mandal, D. Banerjee , *ApJ Letters*. **830**:L33 (2016);
S. mandal et al *A&A* **601**, A106 (2017)
- [45] E.A. Bruevich, G.V. Yakunina, arxiv: 1711.06262
- [46] P. G. Judge, L. Kleint, A. Donea, A. Sainz Dalda and L. Fletcher, *ApJ* **796**, 85 (2014)
- [47] S.A. Matthews et al., *ApJ*. **812** 35 (2015)